J. Res. Inst. Catalysis, Hokkaido Univ., Vol. 13 No. 2, pp. 77 to 101 (1965)

HYDROGEN EVOLUTION REACTION ON SILVER IN ALKALINE SOLUTION

By

Tadayoshi YAMAZAKI*) and Hideaki KITA*)

(Received September 15, 1965)

Abstract

Hydrogen electrode of silver was observed in alkaline solution with a view to verifying the catalytic mechanism previously concluded as operative, by observing the saturation current density at higher cathodic polarization as predicted by the mechanism.

The current density was observed, over the range from 10^{-5} to 10 A cm^{-2} in 1.11 ± 0.01 or 0.26 ± 0.01 N NaOH solution at $21 \pm 2°C$, by applying constant current by pulse technique for a time interval long enough to secure a constant overvoltage toward the end of the pulse but short enough practically to exclude local heating of electrode and local change of electrolyte concentration, which might disturb the observation.

Three different kinds of electrodes were prepared from silver wire of four nine purity, *i.e.* (A) a small sphere formed by heating the silver wire up to melting in helium and enclosed in a thin glass bulb with hydrogen, (B) the wire sealed into glass tube with the sealed end of the latter coated with Araldite, and (C) the wire mounted in Teflon holder with Neoflon; they are referred to below as electrode (A), (B) and (C) respectively. Small glass bulb of electrode (A) was broken in electrolyte solution, while electrodes (B) and (C) were subjected to anodic and cathodic polarizations repeated alternately several times (anodic activation) in the electrolyte solution, respectively immediately before measurements.

Results obtained are as follows.

(1) The current density of one and the same electrode of each kind was observed reproducibly within 10 mV at each overvoltage below the current density of 1 A cm^{-2}. (2) Several tens pieces of electrodes of each kind were submitted to the observation. Best coincident results were obtained along with the least rest-potentials within a few mV as referred to the reversible hydrogen electrode in the same environment with electrode (C), which was used throughout the present research. (3) The decay curve of anodic polarization presents three distinct plateaus respectively at 1.1, 1.4 and 1.6 V as referred to the reversible hydrogen electrode in the same environment, which was observed with a view to investigating the effect of anodic activation mentioned above. (4) TAFEL line of the electrode (C) consists, over the current density below 1 A cm^{-2}, of two linear parts at lower and higher current densities with slope 43 ± 2 mV and 309 ± 5 mV respectively. (5) Beyond the current density of 1 A cm^{-2}, the overvoltage starts to deviate from the TAFEL line, increasing very rapidly with increase of current density,

*) The Research Institute for Catalysis, Hokkaido University, Sapporo, Japan

indicating the saturation current density at about 10 A cm^{-2}. (6) Effect of concentration change from 0.26 to 1.11 N on overvoltage is imperceptible within experimental errors.

The above mentioned results (4) and (5) were theoretically reproduced on the basis of the catalytic mechanism, taking account of the repulsive interactions of hydrogen adatoms each other and between them and a critical complex of the rate-determining step, *i.e.* the recombination of hydrogen adatoms, assuming the predominant contribution to the current density to be due to (111)-lattice plane by analogy with a previous result of exact calculation in case of the hydrogen electrode of nickel.

The present results establish the previous conclusion that the catalytic mechanism is operative on hydrogen electrode of silver.

Introduction

Three mechanisms have so far been advanced for the hydrogen evolution reation,

$$2H^{+} + 2e^{-} = H_2 , \qquad (1)$$

where H^{+} is proton attached to a BRÖNSTED base, H_2O or OH^{-}, and e^{-} is metal electron ; they are

(1) *slow discharge mechanism*, where the discharge of proton

$$H^{+} + e^{-} \xrightarrow{\text{A}} H(a) ,$$

which determines the rate as indicated by symbol $\xrightarrow{\text{A}}$, is followed by the rapid recombination of hydrogen adatoms, H(a)'s,

$$2H(a) \longrightarrow H_2$$

or by the step

$$H^{+} + H(a) + e^{-} \longrightarrow H_2 ,$$

(2) *catalytic mechanism*, where the rapid discharge

$$H^{+} + e^{-} \longrightarrow H(a) \qquad (2.\text{a})$$

is followed by the rate-determining recombination

$$2H(a) \xrightarrow{\text{A}} H_2 , \qquad (2.\text{b})$$

and (3) *electrochemical mechanism*, where the rapid formation of hydrogen molecule-ion, $H_2^{-}(a)$, adsorbed on the electrode,

$$2H^{+} + e^{-} \longrightarrow H_2^{+}(a)$$

is followed by the rate-determining neutralization of $H_2^{+}(a)$

$$H_2^{-}(a) + e^{-} \xrightarrow{\text{A}} H_2 .$$

A number of works have been contributed to the hydrogen electrode of silver in acidic solutions[1~12] but only a few to that in alkaline solutions.[13,14] BOCKRIS *et al.*[13] estimated the adsorbed amount of H(a) on silver electrode in alkaline solution by analyses of galvanostatic transients of the electrode which was preliminarily subjected to polarization of different magnitudes, concluding the slow discharge mechanism as operative. AMMAR and AWAD[14] drew the same conclusion from the value of TAFEL slope of 2RT/F and the value *ca.* 1 of λ, *i.e.* the number of electrons transferred by one act of the rate-determining step. HORIUTI *et al.*[15,16] concluded the catalytic mechanism from the value 6 of the electrolytic separation factor of deuterium[17] and hence predicted the existence of the cathodic saturation current density.[16,18,19]

The saturation current density is understood as concluded necessarily from the catalytic mechanism as follows. The step (2. a) is in the partial equilibrium in this case, which is stated as

$$\mu^{H^+} + F\eta = \mu^{H(a)}$$

in terms of overvoltage, η*), and electrochemical potential, μ^{H^+}, and chemical potential, $\mu^{H(a)}$, respectively of H^+ and H(a). The $\mu^{H(a)}$ increases along with η according to the above equation, which results in the increase of coverage, θ, of H(a). The θ increases, however, just up to unity, where the rate-determining recombination has the constant rate of "decomposition" of a constant system consisting of the electrode fully covered by H(a)'s irrespective of η**). It follows that the specific rate of hydrogen evolution tends to a constant value as called the saturation current density with increase of η toward sufficiently high a value. Such a limiting value is not, however, expected in case of the slow discharge or the electrochemical mechanism. Another conclusion from the catalytic mechanism is the independence of current density against overvoltage on pH.

The cathodic current density of hydrogen electrode of silver in alkaline solution of different concentrations is thus experimentally followed up to the highest possible value of η with a view to verifying the above conclusions from the catalytic mechanism.

---

*) Overvoltage is defined as the negative of the potential of test electrode referred to the reversible hydrogen electrode in the same environment, hence expressed in terms of electrochemical potential, μ^{e^-} or $\mu^{e^-}_{eq}$, of electron in the respective electrodes, as

$$F\eta = \mu^{e^-} - \mu^{e^-}_{eq}.$$

**) In the neighborhood of full coverage, $\mu^{H(a)}$ varies with θ as $\mu^{H(a)} = RT \ln \frac{\theta}{1-\theta} + \text{const}$ (Ref. 18), so that $\mu^{H(a)}$ increases without limit along with the approach of θ to unity, leaving θ practically constant.

Most of the works on the hydrogen electrode of silver have been conducted in the range of current density up to 10^{-2} A cm^{-2}, except those of BOCKRIS *et al.*[4,6], who followed it to the extent of 10^{2} A cm^{-2} (cf. Fig. 7). The results of those works show, however, no sign of the saturation current density at all.

In the present work, local heating and local change of electrolyte concentration are avoided by means of the pulse technique which produces the highest constant current of 1 A. Special precautions are taken to secure the smallest possible value of rest-potential as referred to the reversible hydrogen electrode in the same environment which is a symptom of sound operation of the hydrogen electrode, its departure from zero indicating an inhibition of hydrogen electrode reaction and a concurrence of other electrode reactions. Little attention has hitherto been paid in this respect.

Experimental procedure and experimental results are described in § 1 and § 2, and the latter are reproduced theoretically on the basis of the catalytic mechanism in § 3, according to the lattice plane model[15,16,18,20] where each metal atom of the lattice plane provides a physically identical site for a hydrogen adatom just above it and a pair of sites forms a seat for a critical complx of the rate-determining step.

§ 1. Experimental

Experimental methods are the same as reported previously.[21~23] The difficulties of local heating of electrode and local change of concentration are overcome, as mentioned in the introduction, by means of a pulse of constant current applied for a period of time which is long enough to allow the potential of the test electrode to a constant value toward the end of the pulse but short enough to restrict the local heating of the electrode to 2 degrees at most and the concentration polarization due to local change of concentration of OH^- in alkaline solution to 20 mV at most, as estimated similarly to previous works[21,22], the restricted values being within experimental errors at the relevant high current density.

1-1. Apparatus, electrode and materials

The apparatus consists of, purification trains for gases, a cell accommodating electrodes, a pulse generator and a recorder of potential of electrodes. The purification trains of gases, the cell and the pulse generator are respectively the same with those reported previously.[21,22] A cathode ray oscilloscope (Syncroscope SS 5302, Preamp SP-15H-A IWASAKI Communication Apparatus Co., LTD., Tokyo) or occasionally an electronic recorder (EPR-2T TOA Electronics Co., LTD., Tokyo) has been used as the recorder.

The test electrodes are prepared in different ways as follows with silver wire of four nine purity as stated by the supplier, TANAKA Noble Metal Co., Tokyo. (A) The silver wire of

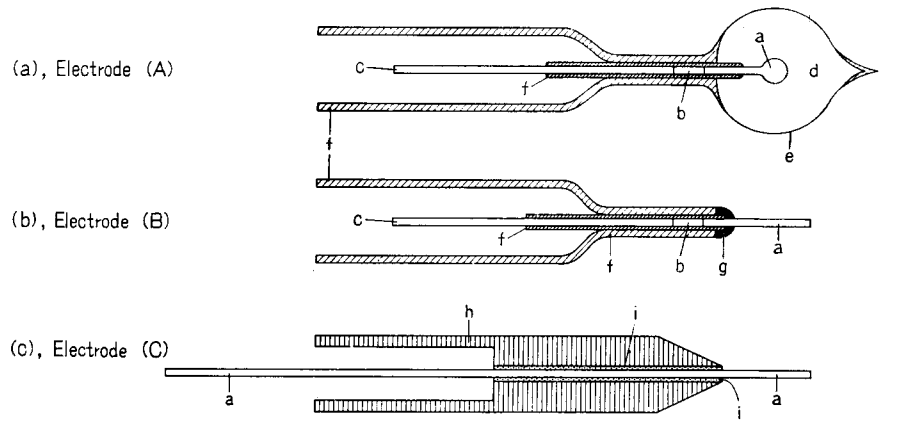

Fig. 1. Diagram of electrode (A), (B) and (C)
a: Ag b: Pt or Ni c: W d: hydrogen atmosphere e: glass bulb
f: glass tube g: Araldite h: Teflon i: Neoflon

0.1 or 0.5 mm diameter is connected to W wire, inserting a piece of Ni- or Pt- wire, between them in order to avoid the difficulty in spot-welding Ag directly to W.[24] W- and Ni- or Pt-wires thus connected and the metal-metal junctions are now covered with *ca.* 0.5 mm thick layer of glass; the juncture of wires thus covered with glass is called a stem in what follows. The stem is now washed with benzene, alcohol, dilute sulfuric acid and conductivity water successively, and the exposed end of wire heated in purified hydrogen gas to reduce its surface oxide and then melted in purified helium gas to form a small sphere at the exposed end of wire, which is sealed in a small glass bulb with hydrogen according to the method of BOCKRIS *et al.*[21~23] (Fig. 1 (a)). These treatments, *i.e.* the reduction in hydrogen, the formation of sphere in helium and the sealing into small glass bulb with hydrogen are conducted without exposing the silver end to air throughout. The glass bulb of the electrode (A) thus prepared is broken in electrolyte solution immediately before measurements. (B) Glass covered part of the stem is fused into a glass tube, and the fused end of the glass tube is covered with Araldite (CIBA Limited, Basle Switzerland) as shown in Fig. 1 (b) for protection against infiltration of solution. The surface of electrode thus prepared is cleaned similarly to the stem in the case of (A). The electrode is now introduced into electrolyte solution and subjected to anodic and cathodic polarizations repeated alternately several times directly before measurements (called anodic activation in what follows). (C) Silver wire is mounted in Teflon holder by means of melted Neoflon (Tetrafluoroethylene-hexafluoropropylene copolymer) as shown in Fig. 1 (c). The electrode is cleaned similarly to the stem of electrode (A) or electrode (B) itself and subjected to the anodic activation similarly to electrode (B) just before the measurement.

Apparent geometrical surface area of the electrodes is either 0.7 or 0.03 cm^2.

The cylinder formed of wire gauze or plate respectively of platinized platinum serves as the counter or the reference electrode. All cocks are water sealed. The apparatus is constructed with borosilicate glass called Hario of SHIBATA Co, LTD., Tokyo. Electrolyte is NaOH from WAKO Pure Chemical Ind., LTD., Osaka or from KANTO Chem. Co., Tokyo; its solution

of 1.11 ± 0.01 or 0.26 ± 0.01 N concentration is reserved in a flask in an atmosphere of purified hydrogen.

1-2. Procedure

Experiment with electrode (A) is conducted as follows. Cell and glass bulb are cleaned with a mixture of 50-50 concentrated nitric and sulfuric acids overnight. Pre-electrolysis is conducted bubbling the purified hydrogen gas through the solution for about 60 hr with current of about 30 mA. The glass bulb is now broken by a glass stick attached to the cell and the spherical test electrode is positioned close to the orifice of the LUGGIN capillary.

Electrode (B) or (C) is cleaned and subjected to the anodic activation immediately before measurements as described in 1-1.

A single pulse of constant current ranging from 10^{-5} to 10 A cm^{-2} is now applied between the test and the cylindrical counter electrodes, the former being situated at the center of the latter. Resulting potential change of the test electrode with time is observed on a screen of the cathode ray oscilloscope and photographed on film (Neopan SSS, FUJI Photo Film Co., LTD.) with a camera (Canon RM, F 1.2). The overvoltage relevant to the applied constant current at the steady state is determined as the constant potential difference between the reference electrode and the test electrode attained toward the end of pulse minus the potential difference due to the solution resistance (called IR drop) between the orifice of the LUGGIN capillary and the test electrode. The IR drop is determined from the initial jump of the potential difference in a very rapid sweep (2μ sec cm^{-1}).[21,22] Solutions are titrated with standard 1.0 or 0.1 N HCl solution after the measurements. All these measurements are carried out at room temperature (21 ± 2°C).

§ 2. Results

2-1. Rest-potential

Rest-potential was measured by an oscilloscope or an electronic recorder referring to the reversible hydrogen electrode in the same environment. E-lectrode (A) showed relatively high an anodic rest-potential amounting 26 ± 11 mV on an average for 73 electrodes and a poor agreement of the $\eta \sim \log i$ relation between them (Fig. 2).

Electrode (B) revealed smaller rest-potential amounting 17 ± 4 mV on an average for 39 electrodes and better agreement of the $\eta \sim \log i$ relation between them (Fig. 3). The higher rest-potential of electrode (A) and its poorer agreement might be due to some sort of contamination induced by the heat treatment as suspected from white powdery appearance of the end of the glass covering near the electrode.

The rest-potential of electrode (C) was measured before and after the measurements of $\eta \sim \log i$ relation, which were found much the same to each other; the values before measurements are shown in the last column of the Table 1. The average value of the rest-potential is 4.5 ± 0.9 mV on an average

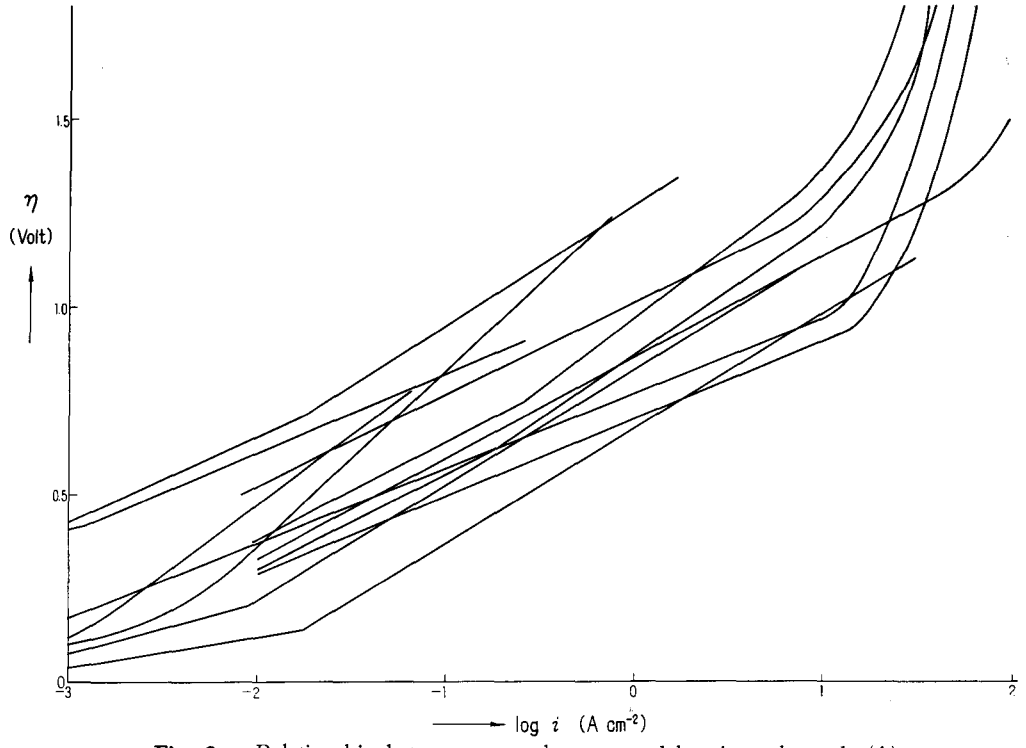

Fig. 2. Relationship between overvoltage, η, and log i on electrode (A).

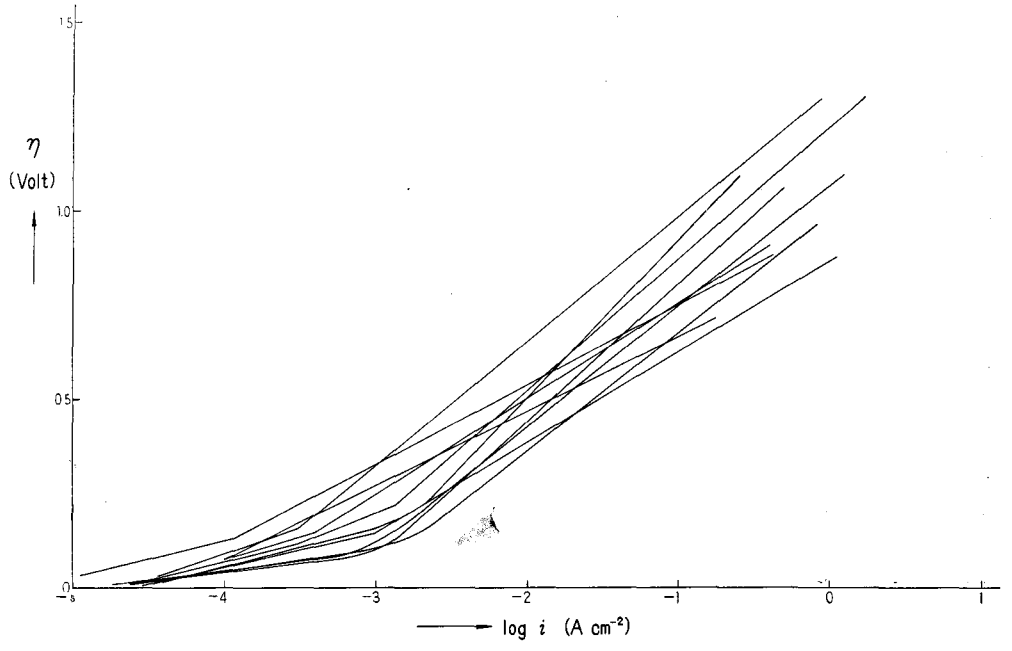

Fig. 3. Relationship between overvoltage, η, and log i on electrode (B).

of 19 electrodes of this kind and a best agreement of $\eta \sim \log i$ relation is obtained between them. Systematic observation was carried out with this kind of electrode as described below.

2-2. Build up and decay curves of anodic polarization

Build up and decay curves of anodic polarization were observed with electrode (C) with a view to investigating the effect of anodic activation. Decay curves of so high an anodic polarization as oxygen evolves, reveal three plateaus, those at 1.4 and 1.1 V, as referred to the reversible hydrogen electrode in the same environment, being well defined as illustrated in Fig. 4. Colour of the electrode surface changes quite sharply from black to light gray along with the decay across 1.4 and then from light gray to slightly yellowish or grayish metallic colour along with the decay across 1.1. This indicates that the plateaus are due to transition of compounds on the surface. The transition is inferred to be that from AgO to Ag_2O, or that from Ag_2O to Ag with reference to the known equilibrium potential 1.4 or 1.1 V[5,26] of the reaction,

$$2AgO + H_2O + 2e^- = Ag_2O + 2OH^- \qquad (3.\ a)$$

or

$$Ag_2O + H_2O + 2e^- = 2Ag + 2OH^- \qquad (3.\ b)$$

respectively. Similar conclusion has been reported by several workers.[27~33] WALES *et al.*[31~33] recently confirmed by X-ray diffraction, the transition of AgO into Ag_2O and the latter into Ag respectively at 1.4 and 1.1 V on the surface of silver electrode at its working condition. The amount of AgO or Ag_2O formed was estimated in accordance with Eq. (3. a) or (3. b) at 10^2 or 5×10^2 layers from the amount of the cathodic current density 10 mA cm^{-2} applied after cessation of the anodic current density of 50 mA cm^{-2} and the length of the respective plateaus on the base of the number of surface atoms of silver assumed to be 10^{15} cm^{-2}. Another plateau observed at 1.6 V indicates also the transition of another higher oxide on the surface, although its amount is much less than those of the other two plateaus. The higher oxide appears to be Ag_2O_3, since the equilibrium potential of the reaction,

$$Ag_2O_3 + H_2O + 2e^- = 2AgO + 2OH^-$$

is known to be 1.5 V[25,26] as referred to the reversible hydrogen electrode in the same environment.

The build up curve of anodic polarization reveals on the other hand only two plateaus before the steady state of oxygen evolution is reached. The first

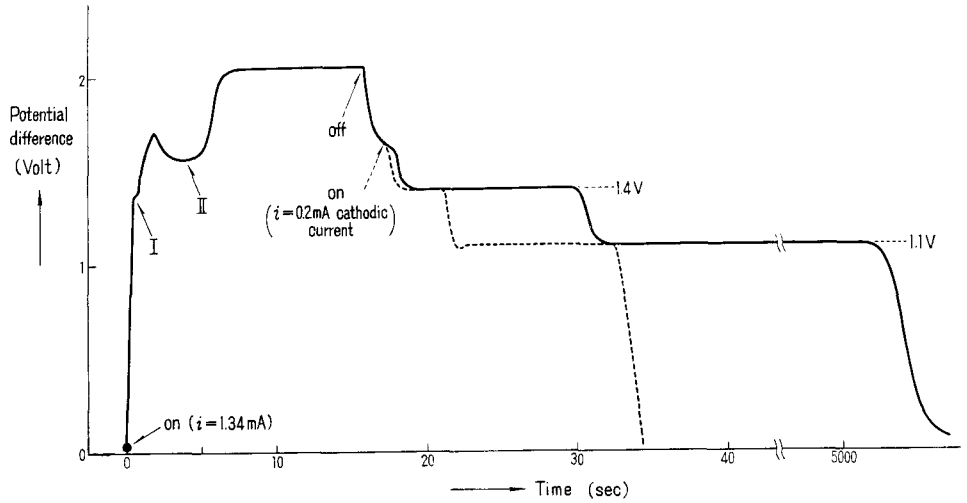

Fig. 4. Build up and decay curves in anodic polarization. Dotted line: the potential change caused by cathodic current applied after anodic polarization.

plateau marked with I in Fig. 4 is much shorter than the second one marked with II indicating much less formation of the lower oxide at the plateau of I, contrary to the findings in the decay curves, which is unexplainable at the moment.

2-3. Build up and decay curves in cathodic polarization

The state of the electrode (C) was further investigated by observation of cathodic and anodic build up as well as decay curves in cathodic region in view of recent results of KABANOV *et al.*[34,35], who suggested the formation of intermetallic compound with alkali metals in alkaline solution on the ground of a plateau as revealed at 1.3 V against a normal hydrogen electrode on the anodic and cathodic build up curves alternately observed in the cathodic region. None of such plateau is now observed in the present experiment but a monotonous change of potential. No intermetallic compound or surface complex needs hence be formed. This difference might be due to that of treatment of electrode; KABANOV *et al.* applied constant high cathodic polarization of 1.2 V against a normal hydrogen electrode for an hour and then that of 1.5~2.0 V for 0.05 sec~2 hr before measurements, whereas the electrode (C) in the present experiment was subjected to the anodic activation for only a few minutes as described above.

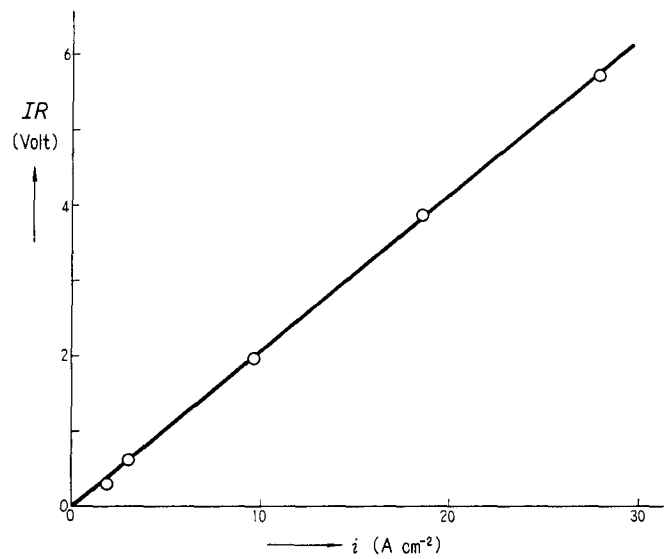

Fig. 5. Relationship between the IR drop and the current density (1.21 N NaOH, 21°C).

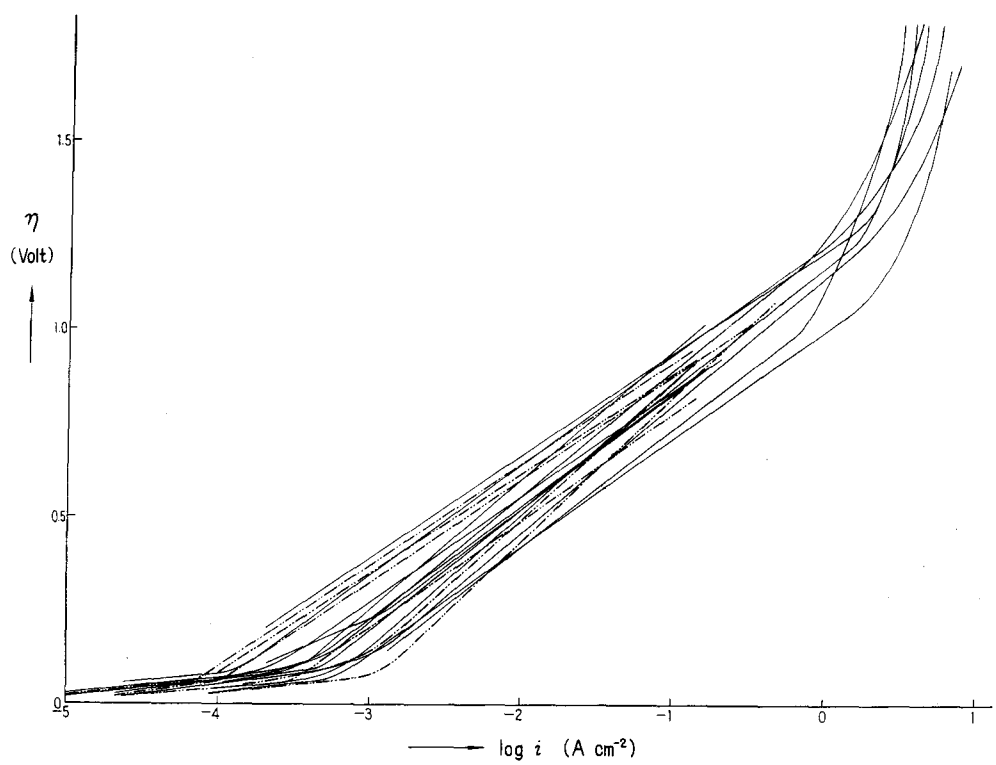

Fig. 6. Relationship between the overvoltage, η, and log i on electrode (C) at 21 ± 2°C.
——: 1.11 ± 0.01 N NaOH ·····: 0.26 ± 0.01 N NaOH

2-4. Roughness factor

The anodic activation was found roughly to treble the differential capacity of the electrode as determined from the initial slope of potential-time curve taken in a very rapid sweep (2μ sec cm^{-1}).[21,22] The current density is thus calculated on the base of roughness factor 3.

2-5. IR drop

A great portion of the total potential difference is the IR drop at higher current densities so that sufficiently accurate determination of it is required for the evaluation of overvoltage. Fig. 5 shows a typical result of IR drop determination (cf. 1-2), plotted against the current density. The precise proportionality of the IR drop to the current density as seen in Fig. 5 confirms the reliability of the IR drop determination.

2-6. $\eta \sim \log i$ relation

Overvoltage, η, determined as described in 1-2 is plotted against log i in Fig. 6. Full or dotted lines represent respectively the results obtained in

TABLE 1 Values of b and i_0 on silver in alkaline solutions.

No.	Conc. of NaOH (N)	b (low) (mV)	b (high) (mV)	i_0 (μA, cm^{-2})	Rest-potential (mV)
1	1.06	50	280	2.28	7.0
2	1.06	50	310	6.66	0.8
3	1.06	30	335	3.94	2.0
4	1.06	40	340	7.52	0.3
5	1.06	52	317	2.14	4.0
6	0.20	38	320	4.66	−0.1
7	0.20	50	390	18.5	22
8	0.20	25	320	2.69	2.0
9	0.29		230	7.07	5.2
10	0.29		370	0.34	0.0
11	0.29	50	280	5.16	3.0
12	0.29	50	295	4.81	1.5
13	0.29	40	275	6.06	4.5
14	0.29	33	260	4.95	0.5
15	1.06		310		10.4
16	1.06		290		32
17	1.06		315		0.2
18	1.06		330		26
19	1.13		340		0.1
20	1.13	53	290		0.6
21	1.26		340		0.2
22	1.21		323		6.3
23	1.21		295		2.3
Mean		43 ± 2	309 ± 5	4.5 ± 0.4	4.5 ± 0.9
Calc.		60	310	5.6	

1.11±0.01 or 0.26±0.01 N NaOH solution at 21±2°C. The curves show two linear parts over the range of current density from 10^{-5} to 1 A cm^{-2}. Values of slopes as well as of exchange current density, i_0, are summarized in Table 1, where i_0 is extrapolated at $\eta=0$ from the linear part of the lower current density. Average value of the slope is 43±2 or 309±5 mV for the part of the lower or higher current densities respectively. These values are remarkably different from the values previously reported as mentioned later.

Beyond the current density of 1 A cm^{-2}, overvoltage starts to deviate from the linear relation and increases quite rapidly around the current density of 10 A cm^{-2} as observed in 1.11 N NaOH solution, indicating the existence of saturation current density thereabouts. Measurements at higher current densities than 1 A cm^{-2} are not conducted in 0.26 N NaOH solution owing to exceedingly large a value of IR drop which renders the determination of overvoltage inaccurate.

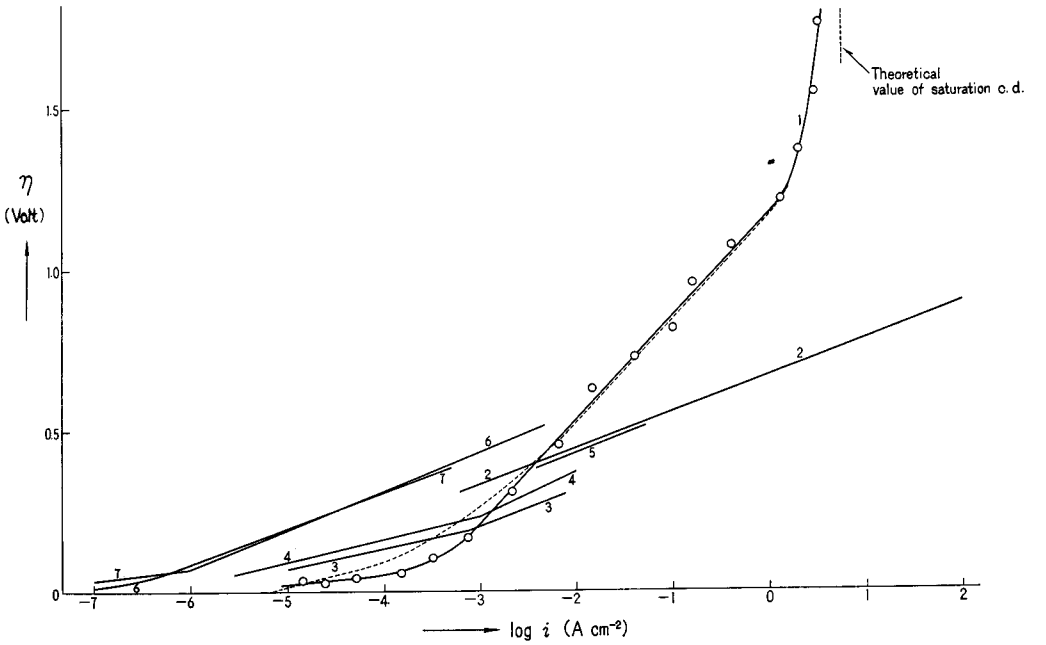

Fig. 7. Comparison of the present results with others.

1) Present results
2) AZZAM and BOCKRIS (5N HCl, 25°C)[4]
3) ANTONIOU and WETMORE (2N H_2SO_4)[10]
4) CONWAY (0.1N HCl, 25°C)[11]
5) GOSSNER, LÖFFLER and SCHWAB (2N H_2SO_4, 18~21°C)[12]
6) DEVANATHAN, BOCKRIS and MEHL (0.1N NaOH, 25°C)[13]
7) AMMAR and AWAD (0.1N NaOH, 30°C)[14]

Dotted line is the theoretical unidirectional rate calculated by Eq. (31).

The $\eta\sim\log i$ relation is not affected by the change of concentration from 1.11 to 0.26 N NaOH within experimental errors as seen from Fig. 6.

2–7. Comparison with previous results

Fig. 7 shows typical one of the present results in comparison with those of other authors both in alkaline and acidic solutions. We see that overvoltage of the present work is lowest at lower current densities and highest at higher current densities. It is the general tendency found in the present experiments that the smaller the rest-potential, the lower the overvoltage is at lower current densities. The rest-potential is in consequence an important characteristic of hydrogen electrode but not at all reported by other authors except by ANTONIOU *et al.*[10], where the rest-potential lies in the range from 350 to 450 mV. The present results are besides remarkably different in revealing the saturation current around 10 A cm^{-2}, from those of BOCKRIS *et al.*[4,6] which indicates no sign of it up to 10^2 A cm^{-2}.

It is now concluded as in the case of nickel[21,22] from the appearance of the saturation current density and the absence of pH effect on $\eta\sim\log i$ relation that the catalytic mechanism is operative on silver in alkaline solution.

§ 3. Theoretical

It is now tried to reproduce the observed $\eta\sim\log i$ relation theoretically on the basis of the catalytic mechanism taking account of the interactions between hydrogen adatoms each other and those between the adatoms and a critical complex. The repulsive potential of an adatom or a critical complex exerted by the surrounding adatoms is here assumed to be proportional to the coverage of hydrogen adatom*). This approximation is called the *proportional* one in what follows.

3–1. Formulation of the reaction rate

Let C be the assembly consisting of electrode, solution and hydrogen gas, and ΩC the partition function of C. The C^I or $C^{\ddagger}$ is defined as the assembly formed by addition of an initial system, I, or a critical complex, $\ddagger$, of a step in question to C and ΩC^I or $\Omega C^{\ddagger}$ as the partition function of C^I or $C^{\ddagger}$ respectively.

According to the theory of reaction rate developed by HORIUTI[16,36,37], the unidirectional rate of the step in question, v_+, is given in general, identifying the transmission coefficient with unity, as

*) This is just the first approximation and a higher approximation will be later conducted as in case of nickel electrode by HORIUTI and one of the present authors[20].

$$v_+ = \frac{kT}{h}\cdot\frac{\mathfrak{Q}C^{\ddagger}}{\mathfrak{Q}C^I} = \frac{kT}{h}\cdot\frac{\mathfrak{Q}C^{\ddagger}/\mathfrak{Q}C}{\mathfrak{Q}C^I/\mathfrak{Q}C} = \frac{kT}{h}\cdot\frac{p^{\ddagger}}{p^I}, \tag{4}$$

where $p^{\ddagger}$ or p^I is the factor with which $\mathfrak{Q}C$ is multiplied by addition of $\ddagger$ or I to form $C^{\ddagger}$ or C^I respectively and k, T or h is of usual meanings. The factor $p^{H(a)}$ is similarly defined as that of multiplication of $\mathfrak{Q}C$ by addition of H(a). The chemical potential, $\mu^{\ddagger}$, μ^I or $\mu^{H(a)}$ of a critical complex, the initial system or hydrogen adatom is now given in terms of $p^{\ddagger}$, p^I or $p^{H(a)}$ respectively as[36,37]

$$\mu^{\ddagger} = -RT\ln p^{\ddagger} \tag{5. a}$$

$$\mu^I = -RT\ln p^I \tag{5. b}$$

or

$$\mu^{H(a)} = -RT\ln p^{H(a)}. \tag{5. c}$$

Eq. (4) is now applied to the rate-determining step of the catalytic mechanism, for which I$\equiv$2H(a). The H(a) is in the partial-equilibrium with H^+ and metal electron, which is expressed in terms of the chemical potential of H(a) and electrochemical potential, μ^{H^+} and μ^{e^-} of H^+ and e^-, as

$$\mu^{H(a)} = \mu^{H^+} + \mu^{e^-} \tag{6. a}$$

or in terms of overvoltage, η, as*)

$$2\mu^{H(a)} = \mu^{H_2} + 2F\eta, \tag{6. b}$$

where μ^{H_2} is the chemical potential of gaseous hydrogen. The factor p^I in Eq. (4) is now given from Eqs. (5. b), (5. c) and (6. b) noting that $\mu^I = 2\mu^{H(a)}$,

$$p_I = \{p^{H(a)}\}^2 = \exp\left(-\frac{\mu^{H_2}+2F\eta}{RT}\right) = p^{H_2}\cdot\exp\left(-\frac{2F\eta}{RT}\right), \tag{7}$$

where p^{H_2} is the BOLTZMANN factor of μ^{H_2} and expressed with good approximation as,

$$p^{H_2} = \frac{Q^{H_2}}{N^{H_2}}, \tag{8}$$

where N^{H_2} is the concentration of hydrogen molecules in gas around the electrode and Q^{H_2} the partition function of a single H_2 molecule in unit volume. Q^{H_2} is given identifying the vibrational partition function with unity, as

$$Q^{H_2} = (2\pi m^{H_2}kT)^{3/2}\cdot 4\pi^2 I_{H_2}kTh^{-5}\cdot\exp\left(-\frac{\varepsilon_g^{H_2}}{RT}\right), \tag{9}$$

*) We have $2\mu^{H^+}+2\mu^{e^-}_{eq}=\mu^{H_2}$ for the reversible hydrogen electrode, hence $2\mu^{H^+}+2\mu^{e^-}-2F\eta=\mu^{H_2}$ in accordance with the equation $F\eta=\mu^{e^-}-\mu^{e^-}_{eq}$ referred to in the footnote on p. 4, or Eq. (6. b) with reference to Eq. (6. a).

where m_{H_2} or I_{H_2} is the mass or the moment of inertia and $\varepsilon_g^{H_2}$ the ground state energy respectively of H_2.

The factor $\Omega C^{\ddagger}/\Omega C$ or $p^{\ddagger}$ in Eq. (4) is given for a group of physically identical seats $\sigma^{\ddagger}$'s as[16,36,37],

$$p^{\ddagger} = \frac{\Omega C^{\ddagger}}{\Omega C} = G^{\ddagger} \frac{\Omega C^{\ddagger}_{\sigma^{\ddagger}(\ddagger)}}{\Omega C}, \tag{10}$$

where $\Omega C^{\ddagger}_{\sigma^{\ddagger}(\ddagger)}$ is the partition function of the assembly $C^{\ddagger}_{\sigma^{\ddagger}(\ddagger)}$, which is the particular case of $C^{\ddagger}$, where the definite one of the physically identical seats of the critical complex is occupied by $\ddagger$ with certainty, and $G^{\ddagger}$ is the total number of $\sigma^{\ddagger}$'s.

The rate expression (4) is now given in terms of forward unidirectional current density, i_+, with reference to Eqs. (7), (8) and (10), as

$$i_+ = \frac{kT}{h} \cdot \frac{2F}{N_A} \cdot \frac{G^{\ddagger}}{A} \cdot \frac{\Omega C^{\ddagger}_{\sigma^{\ddagger}(\ddagger)}}{\Omega C} \cdot \frac{N^{H_2}}{Q^{H_2}} \cdot \exp\left(\frac{2F\eta}{RT}\right), \tag{11}$$

where F is the FARADAY, N_A the AVOGADRO's number, A the surface area and the factor 2 cares for the two elementary charges transferred for every occurrence of step (2. b).

It is now required to evaluate the factor $\Omega C^{\ddagger}_{\sigma^{\ddagger}(\ddagger)}/\Omega C$ as a function of η in order to derive i_- as a function of η according to Eq. (11). It has been shown with f.c.c. crystal of nickel[16,20] by theoretical calculation that contribution to i_- of the critical complex in $\sigma^{\ddagger}$, provided by a pair of metal atoms in the closest distance, 2.49 Å, on (111)-lattice plane, predominates over that of critical complex in $\sigma^{\ddagger}$ provided by any other possible pair of metal atoms on any principal lattice plane, *i.e.* $2.49\sqrt{3}$ Å distant one on (111)-, 2.49 or $2.49\sqrt{2}$ Å distant one on (100)- or 2.49, $2.49\sqrt{2}$ or $2.49\sqrt{3}$ Å distant one on (110)-lattice plane. Hence by analogy, the present rough calculation with the f.c.c. crystal of silver is conducted with $\sigma^{\ddagger}$ provided by a pair of the metal atoms in the closest distance of 2.883 Å on (111)-lattice plane.

3-2. Configuration of critical complex

The factor $\Omega C^{\ddagger}_{\sigma^{\ddagger}(\ddagger)}/\Omega C$ in Eq. (11) is now evaluated by working out first the configuration of the critical complex from adiabatic potential of the system consisting of two hydrogen atoms and two metal atoms, the latter being fixed at a distance of 2.883 Å. COULOMB and exchange energies, K and J, are determined as before[16,18,20] from the MORSE function,

$$K+J = D\left[\exp\{-2a(r-r_0)\} - 2\exp\{-a(r-r_0)\}\right] \tag{12}$$

TABLE 2 Numerical values of constants of MORSE function and the percentage of COULOMb energy.

	D (Kcal mol^{-1})	a (Å^{-1})	r_0 (Å)	$K/(K+J)$
H-H	109	1.98	0.7395	11%
Ag-H	57.658	1.508	1.6174	26%
Ag-Ag	18.6			41%

and the percentage of the COULOMB energy comprised in the MORSE function, the latter being calculated by SLATER, ROSEN and IKEHARA's method.[38,39] Table 2 shows the numerical values of the constants in Eq. (12) and of the above percentage for the respective pair of atoms.

The potential energy, ε^*, of the system around the critical state is now expressed as

$$\begin{aligned}\varepsilon^* = {} & K_{Ag(1)-Ag(2)} + K_{H(1)-H(2)} + K_{Ag(1)-H(1)} + K_{Ag(2)-H(1)} \\ & + K_{Ag(1)-H(2)} + K_{Ag(2)-H(2)} \\ & - \left[\frac{1}{2}\left\{(J_{Ag(1)-Ag(2)} + J_{H(1)-H(2)} - J_{Ag(1)-H(2)} - J_{Ag(2)-H(1)})^2\right.\right. \\ & + (J_{Ag(1)-Ag(2)} + J_{H(1)-H(2)} - J_{Ag(1)-H(1)} - J_{Ag(2)-H(2)})^2 \\ & \left.\left. + (J_{Ag(1)-H(1)} + J_{Ag(2)-H(2)} - J_{Ag(2)-H(1)} - J_{Ag(1)-H(2)})^2\right\}\right] \\ & + \sum_j \left(K_j - \frac{1}{2} J_j\right), \end{aligned} \tag{13}$$

where the last term $\sum_j \left(K_j - \frac{1}{2} J_j\right)$ is the potential of repulsions exerted upon the pair of two hydrogen atoms constituting a critical complex by surrounding silver atoms on the (111)-lattice plane. Summation was taken over the metal atoms situated 2.883 and $2.883\sqrt{3}$ Å apart from any of the two metal atoms providing the σ^*. Calculated results are expressed in terms of coordinates, *i.e.*

$$\begin{aligned} x &= (x_1 + x_2)/2\,, \qquad y = (y_1 + y_2)/2\,, \qquad z = (z_1 + z_2)/2\,, \\ \bar{x} &= (x_2 - x_1)/2\,, \qquad \bar{y} = (y_2 - y_1)/2\,, \qquad \bar{z} = (z_2 - z_1)/2\,, \end{aligned}$$

where (x_1, y_1, z_1) and (x_2, y_2, z_2) are rectangular coordinates of the individual hydrogen atoms as illustrated in Fig. 8; x_1 or x_2 is the distance of hydrogen atom, 1 or 2, from the lattice plane (YZ plane in Fig. 8), y_1 or y_2 the distance from the plane (ZX in Fig. 8) bisecting perpendicularly the line combining the two metal atoms and z_1 or z_2 the distance from a plane (XY in Fig. 8), which is perpendicular to the lattice plane and comprises the two metal atoms. The x is thus the height of the center of the two hydrogen atoms above the lattice

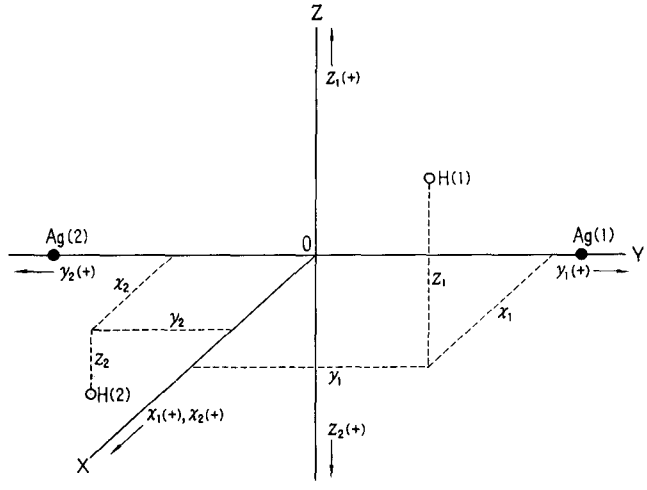

Fig. 8. Coordinates of two hydrogen atoms. *YZ* plane represents the lattice plane.

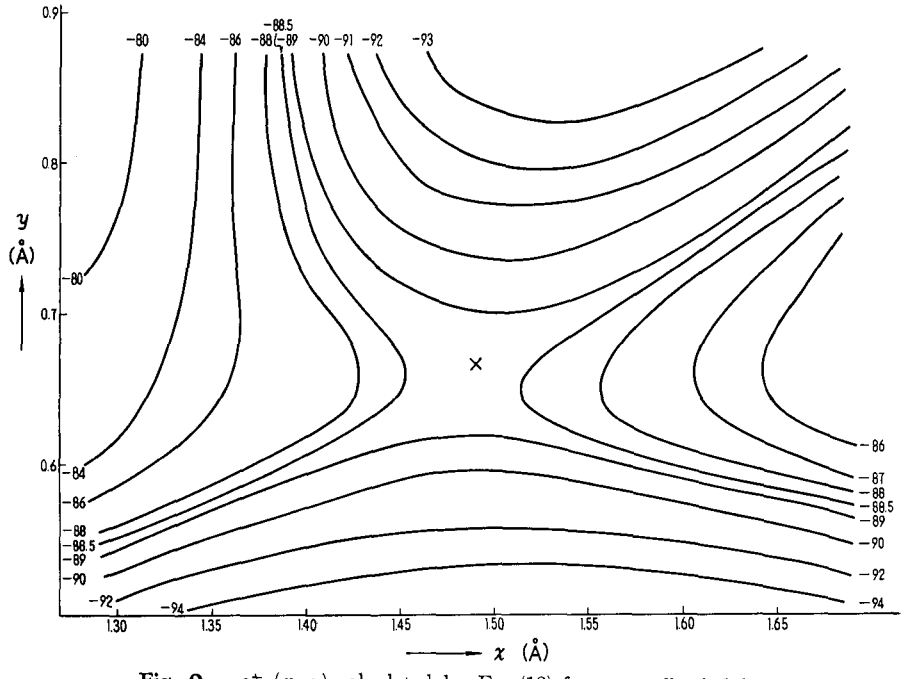

Fig. 9. ε^* (x, y) calculated by Eq. (13) for seat afforded by a pair of 2.883 Å spaced metal atoms on (111)-lattice plane. Energy is referred to that of the state where four atoms are at rest infinitely apart from each other. X indicates the saddle pont.

plane and y or z is the half of the sum of distances from the plane ZX or XY respectively.

The potential energy has the extreme value with reference to z, $\bar{x}$, $\bar{y}$, and $\bar{z}$ at $z=\bar{x}=\bar{y}=\bar{z}=0$ as required by the symmetry of the configuration and is particularly a minimum with respect to z, $\bar{x}$, $\bar{y}$, and $\bar{z}$ according to Eq. (13). The value of ε at the above minimum is illustrated as a function of x and y in Fig. 9, where ε^* less the last term of Eq. (13), *i.e.* the energy of the four atoms is referred to that of the state where the four atoms are at rest infinitely apart from each other. Saddle point is determined at $x=1.49$ Å, $y=0.67$ Å from Fig. 9. The ε^* is now expanded in TAYLOR's series around the saddle point in order to evaluate the vibrational frequencies, ν^*'s, as,

$$\varepsilon^* = \varepsilon_0^* + \sum^{x\cdots\bar{z}} \frac{a_{xx}}{2}(x-x_0)^2 + a_{xy}(x-x_0)(y-y_0) + a_{\bar{z}\bar{y}}\bar{x}\bar{y}\,, \tag{14}$$

where ε_0^* is the value of ε^* at the saddle point and a_{xx}, *etc.* are the force constants. Other cross terms vanish on account of the symmetry. The frequencies were determined by the following equations, into which the sixth order secular equation derived from Eq. (14) separates, *i.e.*

$$(a_{xx}-2m_H\lambda)(a_{yy}-2m_H\lambda)-a^2_{xy}=0$$
$$(a_{\bar{x}\bar{x}}-2m_H\lambda)(a_{\bar{y}\bar{y}}-2m_H\lambda)-a^2_{\bar{x}\bar{y}}=0$$
$$a_{zz}-2m_H\lambda=0$$

and

$$a_{\bar{z}\bar{z}}-2m_H\lambda=0\,,$$

where m_H is the mass of hydrogen atom and $\lambda=4\pi^2(\nu^*)^2$. Results are shown in Table 3. One of the six values is imaginary, which corresponds to the reaction path.

Vibrational frequencies of hydrogen adatoms are determined by the equations ;

$$\nu_x = \frac{[(\partial^2\varepsilon^H/\partial x^2)_{x=x_0}]^{1/2}}{2\pi m^{1/2}}\,,\quad \nu_y = \frac{[(\partial^2\varepsilon^H/\partial y^2)_{y=0}]^{1/2}}{2\pi m^{1/2}}\,,\quad \nu_z = \frac{[(\partial^2\varepsilon^H/\partial z^2)_{z=0}]^{1/2}}{2\pi m^{1/2}}\,, \tag{15}$$

where the potential energy of hydrogen adatom, ε^H, is expressed as,

$$\varepsilon^H = D_{Ag-H}\left[\exp\{-2a_{Ag-H}(r-r_0)\}-2\exp\{-a_{Ag-H}(r-r_0)\}\right] + \sum_j\left(K_j-\frac{1}{2}J_j\right), \tag{16}$$

the last term being the sum of the potentials of exerted upon the hydrogen

TABLE 3 Vibrational frequencies of hydrogen adatom and critical complex on (111)-lattice plane of silver.

ν_i (cm^{-1})	1241	134	134			
$\nu_j^{\ddagger}$ (cm^{-1})	1254.9	1470.6	520.7	546.5	230.2	1647.5 i

adatom by the surrounding metal atoms on the (111)-lattice plane. Table 3 shows the values of $\nu^{\ddagger}$'s, ν_x *etc.* thus worked out.

3-3. $\Omega C^{\ddagger}_{\sigma^{\ddagger}(\ddagger)}$ and ΩC

Based on the results of the preceding sections, the factor $\Omega C^{\ddagger}_{\sigma^{\ddagger}(\ddagger)}/\Omega C$ in Eq. (11) is calculated for a critical complex in $\sigma^{\ddagger}$ provided by a pair of metal atoms 2.883 Å apart from each other on (111)-lattice plane, taking account of the repulsion due to surrounding hydrogen adatoms by the proportional approximation.

ΩC; According to the properties of partition function, ΩC is given as the sum of $\Omega C_{\sigma_i(0)}$ and $\Omega C_{\sigma_i(H)}$, *i.e.*

$$\Omega C = \Omega C_{\sigma_i(0)} + \Omega C_{\sigma_i(H)} , \tag{17}$$

where $\Omega C_{\sigma_i(0)}$ or $\Omega C_{\sigma_i(H)}$ is the partition function of the assembly C at a particular state, $C_{\sigma_i(0)}$ or $C_{\sigma_i(H)}$, where a particular site σ_i is kept unoccupied or occupied by a hydrogen adatom respectively with certainty.

Let now σ_i be either of the two constituent sites of $\sigma^{\ddagger}$, say, σ_1. The $\Omega C_{\sigma_1(H)}$ or $\Omega C_{\sigma_1(0)}$ is then developed with reference to $\sigma^{\ddagger}$ as,

$$\Omega C_{\sigma_1(H)} = \Omega C_{\sigma^{\ddagger}\{\sigma_1(H),\sigma_2(0)\}} + \Omega C_{\sigma^{\ddagger}\{\sigma_1(H),\sigma_2(H)\}} \tag{18}$$

or

$$\Omega C_{\sigma_1(0)} = \Omega C_{\sigma^{\ddagger}\{\sigma_1(0),\sigma_2(0)\}} + \Omega C_{\sigma^{\ddagger}\{\sigma_1(0),\sigma_2(H)\}} , \tag{19}$$

where $\Omega C_{\sigma^{\ddagger}\{\sigma_1(H),\sigma_2(0)\}}$ is the partition function of the assembly of C at the particular state, $C_{\sigma^{\ddagger}\{\sigma_1(H),\sigma_2(0)\}}$, where σ_1 is occupied by a hydrogen adatom and the other constituent site σ_2 of $\sigma^{\ddagger}$ is unoccupied. Definitions of the other partition functions on the right hand side of the above two equations are similarly understood according to the parenthesized suffixes. These partition functions are formulated taking account of repulsions due to surrounding hydrogen adatoms by the proportional approximation in accordance with spacing shown in Fig. 10 (a), of sites near $\sigma^{\ddagger}$ on (111)-lattice plane, as

$$\begin{aligned}
&\Omega C_{\sigma^{\ddagger}\{\sigma_1(H),\sigma_2(0)\}} = \Omega C_{\sigma^{\ddagger}(0)} \gamma I_\theta^5 III_\theta^6 \\
&\Omega C_{\sigma^{\ddagger}\{\sigma_1(H),\sigma_2(H)\}} = \Omega C_{\sigma^{\ddagger}(0)} \gamma^2 II_\theta^{10} III_\theta^{12} \\
&\Omega C_{\sigma^{\ddagger}\{\sigma_1(0),\sigma_2(0)\}} = \Omega C_{\sigma^{\ddagger}(0)} \\
&\Omega C_{\sigma^{\ddagger}\{\sigma_1(0),\sigma_2(H)\}} = \Omega C_{\sigma^{\ddagger}(0)} \gamma I_\theta^5 III_\theta^6 ,
\end{aligned} \tag{20}$$

where $\Omega C_{\sigma^*(0)}$ is the partition function of the assembly C^* at the particular state, *i.e.* $C_{\sigma^*(0)}$, where a particular seat σ^* is kept unoccupied, γ the BOLTZMANN factor of the reversible work required to transfer a hydrogen atom from its adsorbed state to the standard state and then from the standard state to a definite, preliminarily evacuated site inside σ^*, less the reversible work due to the repulsions with surrounding hydrogen adatoms in the latter process. I_θ, III_θ, or I is the BOLTZMANN factor of the repulsive potential, $R_I\theta$, $R_{III}\theta$, or R_I respectively, *i.e.*

$$I_\theta = \exp(-R_I\theta/RT)\,,$$
$$III_\theta = \exp(-R_{III}\theta/RT)\,,$$
$$I = \exp(-R_I/RT)\,, \qquad (21.\text{a})$$

where R_I or R_{III} is the repulsive potential of the hydrogen adatom of interest due to the one $2.883\sqrt{3}$ Å apart from the former, which is taken α times*) as large as -35%[16,18,20] of the MORSE function of hydrogen molecule, *i.e.*

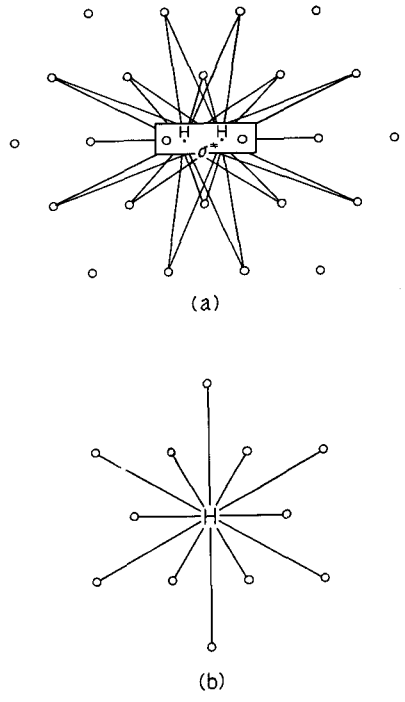

Fig. 10. Interactions of critical complex (a) or hydrogen adatom (b) with surrounding silver atoms on (111)-lattice plane.

$$R_I = 1.086\,\alpha\,, \qquad R_{III} = 0.0168\,\alpha\ (\text{Kcal mole}^{-1})\,, \qquad (21.\text{b})$$

where α is the parameter to be adjusted. The γ defined above is expressed as,

$$\gamma = q_0^{H(a)}/p^{H(a)}\,, \qquad (22)$$

where $q_0^{H(a)}$ is the BOLTZMANN factor of the reversible work required to transfer a hydrogen atom from its standard state to a definite, preliminarily evacuated site less the part due to interactions. The $q_0^{H(a)}$ is given as[16]

$$q_0^{H(a)} = \prod_{j=1}^{3}\left\{1-\exp\left(-h\nu_j/kT\right)\right\}^{-1}\cdot\exp\left(-\varepsilon_g^{H(a)}/RT\right)\,, \qquad (23)$$

*) It has been concluded by TOYA in terms of first principles of quantum mechanics[40,41] that the repulsion between adatoms must be greater than the exchange repulsion between hydrogen atoms not bounded with each other and actually shown[42] from the analysis of hydrogen isotherm on nickel that the repulsive potential among hydrogen adatoms is larger than the exchange repulsive potential estimated as -35% of the MORSE function.

where ν_j is the frequency of the j-th normal mode of vibration of the hydrogen adatom and $\varepsilon_g^{H(a)}$ is its energy in the ground state. Hence, we have from Eqs. (7), (8), (9), (22) and (23),

$$\gamma = \frac{q_0^{H(a)}}{p^{H(a)}} = \sqrt{\frac{N^{H_2}h^5}{(2\pi m_{H_2}kT)^{3/2}\cdot 4\pi^2 I_{H_2}kT}} \cdot \prod_{j=1}^{3}\left\{1-\exp\left(-\frac{h\nu_j}{kT}\right)\right\}^{-1} \exp\left(-\frac{\frac{1}{2}\varepsilon_g^{H_2}-\varepsilon_g^{H(a)}+F\eta}{RT}\right) \tag{24. a}$$

or

$$\gamma = 1.003\cdot 10^{-2}\exp\left(-\frac{\frac{1}{2}\varepsilon_g^{H_2}-\varepsilon_g^{H(a)}+F\eta}{RT}\right) \tag{24. b}$$

at 25°C and 1 atmospheric pressure of hydrogen gas, using numerical values of $m_{H_2}=3.337\times 10^{-24}$ and $I_{H_2}=4.664\times 10^{-41}$ g cm^2. ΩC is now given from Eqs. (17), (18), (19) and (20) as

$$\Omega C = \Omega C_{\sigma^*(0)}(1+2\zeta+I\zeta^2), \tag{25}$$

where

$$\zeta = \gamma I_\theta^5 III_\theta^6. \tag{26}$$

$\Omega C^*_{\sigma^*(*)}$; $\Omega C^*_{\sigma^*(*)}$ is similarly formulated as

$$\Omega C^*_{\sigma^*(*)} = \Omega C_{\sigma^*(0)} q_0^* \zeta^*, \tag{27}$$

where q_0^* is the BOLTZMANN factor of the reversible work required to transfer two hydrogen atoms from their standard state to a definite, preliminarily evacuated seat σ^* less the part due to interactions with surrounding hydrogen adatoms. The q_0^* is now given as

$$q_0^* = \exp\left(-\frac{\varepsilon_g^*}{RT}\right)\cdot\prod_{i=1}^{5}\left\{1-\exp\left(-\frac{h\nu_i^*}{RT}\right)\right\}^{-1},$$

where ν_i^* is the frequency of the i-th normal mode of vibration of a critical complex and ε_g^* its energy at the ground state. ζ^* in Eq. (27) is the BOLTZMANN factor of the excess of the reversible work required to bring up constituent hydrogen atoms of a critical complex from their standard state onto the definite, preliminarily evacuated seat, due to the repulsion exerted by surrounding hydrogen adatoms which is taken $R^*\theta$ by the proportional approximation, *i. e.*

$$\zeta^* = \exp(-R^*\theta/RT), \tag{28}$$

where the proportionality constant, R^*, is a parameter to be adjusted.

3-4. Rate

The factor $\Omega C^{*}_{\sigma^{*}(*)}/\Omega C$ in the rate equation (11) is now expressed by Eqs. (25) and (27) as

$$\Omega C^{*}_{\sigma^{*}(*)}/\Omega C = q_0^{*}\cdot\zeta^{*}/(1+2\zeta+I\zeta^2) \tag{29}$$

hence, referring to Eqs. (9) and (28),

$$i_{+} = \frac{2FkTN^{H_2}G_1^{*}\cdot\exp\{-(\varepsilon_g^{*}-\varepsilon_g^{H_2})/RT\}}{N_A(2\pi m_{H_2}kT)^{3/2}\cdot 4\pi^2 I_{H_2}kT\cdot\prod_{i=1}^{5}\{1-\exp(-h\nu_i^{*}/RT)\}}\cdot\frac{\zeta^{*}}{(1+2\zeta+I\zeta^2)}\cdot\exp\left(\frac{2F\eta}{RT}\right) \tag{30}$$

where

$$G_1^{*} = G^{*}/A = 4.2\times 10^{15}\ \mathrm{cm}^{-2}$$

as follows from the geometry of the (111)-lattice plane. We have from Eq. (30) at 25°C and 1 atmospheric pressure of hydrogen

$$i_{+} = 7.406\cdot 10^{4}\cdot\exp\{-(\varepsilon_g^{*}-\varepsilon_g^{H_2})/RT\}\cdot\exp\left(\frac{2F\eta}{RT}\right)\cdot\frac{\zeta^{*}}{(1+2\zeta+I\zeta^2)}, \tag{31}$$

where ζ^{*} and ζ are the functions of the coverage, θ, of hydrogen adatom as seen from Eqs. (28), (26) and (21. a). It is now required to determine θ as a function of η for working out i_{+} as such.

In accordance with the lattice plane model[16,20,42], all sites on (111)-lattice plane are physically identical with each other, hence the coverage of hydrogen adatoms is identical with the probability of σ_i being occupied by a hydrogen adatom, *i.e.* in terms of partition functions defined above,

$$\theta = \Omega C_{\sigma_i(H)}/\Omega C$$

hence with reference to Eq. (17)

$$\theta/(1-\theta) = \Omega C_{\sigma_i(H)}/\Omega C_{\sigma_i(0)}\,. \tag{32}$$

The partition function $\Omega C_{\sigma_i(H)}$ is written by the proportional approximation as

$$\Omega C_{\sigma_i(H)} = \Omega C_{\sigma_i(0)}\cdot\gamma\cdot\xi \tag{33}$$

where ξ is the BOLTZMANN factor of the excess of the reversible work required to transfer a hydrogen atom from its standard state to the preliminarily evacuated site σ_i, due to interaction with surrounding hydrogen adatoms; ξ is approximated counting as such only those on the sites 2.883 and $2.883\sqrt{3}$ Å apart from σ_i, which are respectively 6 in number on (111)-lattice plane as seen from Fig.

10. (b), as

$$\xi = \exp\left\{-\frac{6(R_I + R_{III})\,\theta}{RT}\right\}. \tag{34}$$

The function $\theta(\eta)$ is now calculated by Eqs. (32), (33), (34) (21. b) and (24. b) at 25°C and 1 atmospheric pressure of hydrogen by trial and error method. Using $\theta(\eta)$ thus evaluated, $i_+(\eta)$ is calculated by Eqs. (31), (28), (25), (21. a), (21. b) and (24. b), where the values of constants, $\varepsilon_g^* - \varepsilon_g^{H_2}$, R^*, α and $\varepsilon_g^{H(\alpha)} - \frac{1}{2}\varepsilon_g^{H_2}$ are adjusted to those given in the next section, which make the theoretical function $i_+(\eta)$ to fit in best with the experimental one.

3–5. Comparison with experimental results

Theoretical value of $i_+(\eta)$ is shown in Fig. 7 on the base of the adjusted values of the parameters, α, *etc.*

$\alpha = 5$

$2\varepsilon_g^{H(\alpha)} - \varepsilon_g^{H_2} = -4.0$ Kcal mole^{-1},

$R^* = 11.3\,\alpha$ Kcal mole^{-1},

$\varepsilon_g^* - \varepsilon_g^{H_2} = 11.2$ Kcal mole^{-1}.

We see a satisfactory agreement of the theoretical results with experimental one. On the other hand, the above adjusted value of $2\varepsilon_g^{H(\alpha)} - \varepsilon_g^{H_2}$ indicates a low heat of adsorption, that of α a high repulsive potentials and the both incorporated specify silver as a poor or practically incompetent adsorbent of hydrogen in accordance with well-known experimental results that hydrogen adsorption on silver is not perceptible.[43]

The value of $\alpha = 5$ obtained here is extraordinary large as compared with $\alpha = 1.5$ previously determined in the case of nickel. This is in conformity with Toya's theory[40,41] of hydrogen adsorption, which states that the repulsive potential between adatoms arising from their competition for metal electrons participating in the bond, increases with decrease of the level density of electron on the Fermi surface, whereas the level density of silver is much smaller than that of nickel as follows from the values of electronic specific heat and magnetic susceptibility.

Conclusive Remarks

Hydrogen evolution reaction of silver was observed in 1.11 ± 0.01 and 0.26 ± 0.01 N NaOH solution at 21 ± 2°C in a range of current density from 10^{-5} to 10 A cm^{-2}. Electrodes were prepared in three different ways and a

number of pieces of electrode of each preparation were subjected to the above investigation. It was found that the best concordant results and the smallest rest-potential, *i.e.* 4.6±0.9 mV as referred to the reversible hydrogen electrode in the same environment were obtained in case of electrodes of the preparation, where silver wire was mounted in Teflon holder by molten Neoflon and subjected to the anodic activation before measurements.

Results obtained with the electrodes are as follows.

(1) TAFEL plot of one and the same electrode is reproducible within 10 mV for current densities below 1 A cm^{-2}.

(2) TAFEL plot splits into two linear parts with slopes 43±2 and 309 ±5 mV respectively at lower and higher current densities.

(3) The cathodic saturation current density is observed at *ca.* 10 A cm^{-2} in 1.11±0.01 N NaOH solution.

(4) The TAFEL plot is affected imperceptibly by concentration change of electrolyte solution from 0.26 to 1.11 N.

From the results (3) and (4) mentioned above, it is concluded that the catalytic mechanism is operative on the hydrogen electrode of silver in alkaline solution.

The observed $\eta \sim \log i$ relation was reproduced theoretically on the basis of the catalytic mechanism taking account of the repulsive interactions by the proportional approximation, assuming the predominant contribution from the (111)-lattice plane of the f. c. c. crystal to the current density on analogy of similar conclusion arrived at by elaborate theoretical calculations on the hydrogen electrode of nickel.

Acknowledgement

The authors wish to express their sincere gratitude to Emeritus Prof. J. HORIUTI for his useful discussions given throughout the prsent work.

References

1) F. P. BOWDEN and E. K. RIDEAL, Proc. Roy. Soc., **A 120**, 59 (1928).
2) *Idem*, *ibid.*, **A 120**, 80 (1928).
3) A. M. AZZAM, J. O'M. BOCKRIS, B. E. CONWAY and H. ROSENBERG, Trans. Faraday Soc., **46**, 918 (1950).
4) A. M. AZZAM and J. O'M. BOCKRIS, Nature, **165**, 403 (1950).
5) J. O'M. BOCKRIS and B. E. Conway, Trans. Faraday Soc., **48**, 724 (1952).
6) J. O'M. BOCKRIS and A. M. AZZAM, *ibid.*, **48**, 145 (1952).
7) M. BREITER, C. A. KNORR and W. VOLKL, Z. Elektrochem., **59**, 681 (1955).
8) H. GERISCHER and W. MEHL, Z. Elektrochem., **59**, 1049 (1955).

9) J. O'M. BOCKRIS, I. A. AMMAR and A. K. M. S. HUQ, J. Phys. Chem., **61**, 879 (1957).
10) A. A. ANTONIOU and F. E. W. WETMORE, Can. J. Chem., **37**, 222 (1959).
11) B. E. CONWAY, Proc. Roy. Soc. (London), **A 256**, 128 (1960).
12) K. GOSSNER, Chr. LÖFFIER and G. M. SCHWAB, Z. Phys. Chem. Neue Folge, **28**, 229 (1961).
13) M. A. V. DEVANATHAN, J. O'M. BOCKRIS and W. MEHL, J. Electroanal. Chem., **1**, (1960).
14) I. A. AMMAR and S. A. AWAD, Phys. Chem., **60**, 1290 (1956).
15) T. KEII, Shokubai, **4**, 55 (1956).
16) G. OKAMOTO, J. HORIUTI and K. HIROTA, Sci. Papers Inst. Phys. Chem. Research (Tokyo), **29**, 223 (1963).
17) J. HORIUTI and G. OKAMOTO, *ibid.*, **28**, 231 (1936).
18) J. HORIUTI, This Journal, **4**, 55 (1956).
19) J. HORIUTI, *Trans. Symposium Electrode Processes*, edited by E. Yeager, John Wiley and Sons, Inc., 1961, p. 17.
20) J. HORIUTI and H. KITA, This Journal, **12**, 122 (1964).
21) H. KITA and T. YAMAZAKI, *ibid.*, **11**, 10 (1963).
22) H. KITA and O. NOMURA, *ibid.*, **12**, 107 (1964).
23) J. O'M. BOCKRIS and H. KITA, J. Electrochem. Soc., **109**, 928 (1962).
24) R. W. ROBERTS and T. A. VANDERSLICE, *Ultrahigh Vacuum and its Applications*, Prentice Hall Inc., 1963, p. 113.
25) W. M. LATIMER, *Oxidation Potentials*, Second Edition, Prentice Hall Inc. 1952.
26) R. PARSONS, *Handbook of Electrochemical Constant*, Butterworths Scientific Publications 1959.
27) G. BIANCHI, G. CAPRIOGLIO, F. MAZZA and T. MUSSINI, Electrochemica Acta, **1**, 232 (1961).
28) T. P. DIRKSE, J. Electrochem. Soc., **107**, 859 (1960).
29) T. P. DIRKSE and J. BARRY de ROOS, Z. Phys. Chem. Neue Folge, **41**, 1 (1964).
30) A. HICKLING and D. TAYLOR, Disc. Faraday Soc., **1**, 277 (1947).
31) C. P. WALES and J. BURBANK, J. Electrochem. Soc., **106**, 885 (1959).
32) *Idem*, *ibid.*, **111**, 1002 (1964).
33) *Idem*, *ibid.*, **112**, 13 (1965).
34) B. N. KABANOV, D. I. LEIKIS, I. G. KISELEVA, I. I. ASTOKHOV and D. P. ALEXANDROVA, Dokl. Akad. Nauk. SSSR, **144**, 1085 (1962).
35) I. G. KISELEVA, N. N. TOMASHOVA and B. N. KAVANOV, Zhur. Fiz. Khim., **38**, 1188 (1964).
36) J. HORIUTI, This Journal, **1**, 8 (1948-51).
37) J. HORIUTI, *Report of IUPAC Commission on Colloid and Surface Chemistry*, 1964.
38) J. C. SLATER, Phys. Rev., **36**, 57 (1930).
39) N. ROSEN and S. IKEHARA, *ibid.*, **43**, 5 (1933).
40) T. TOYA, This Journal, **6**, 308 (1958).
41) *Idem*, *ibid.*, **8**, 209 (1960).
42) J. HORIUTI and T. TOYA, *ibid.*, **12**, 76 (1964).
43) G. C. BOND, *Catalysis by Metals*, Academic Press Inc. London, 1962.